Impacts of climate change on the growing season in the Iran

Behroz Sari Sarraf[1], Ali Mohammad Khorshiddost[1], Peyman Mahmoudi[*2], Mohammad Daraei[1]*

Abstract: *This study addresses the impact of global warming on temporal-spatial changes in growing season in Iran in the coming decades using daily data from 43 meteorological stations of the country during the time period of 1981-2010. Data for future periods were simulated in LARS-WG ed.5 using the outputs of two atmospheric general circulation models (HadCM3 and GFCM21) and three emission scenarios (A2, B1, and A1B). Analysis of future temperature conditions suggests a greater increase in minimum temperature compared to maximum temperature across Iran. Compared to the growing season of 1981-2010, the results based on the GFCM21 model for A2, A1B, and B1 emission scenarios showed that the length of growing season in the time span of 2046-2065 will be extended by 21, 19 and 13 days respectively. Based on the HadCM3 model and the aforementioned scenarios, the average increase in the length of growing season in Iran is 18, 17 and 14 days respectively. The GFCM21 model predicts the growing season to be extended by 29, 32 and 17 days in during the period of 2080-2099. The average extension of growing season in HadCM3 model compared to the period of observation is 28, 34 and 20 days.*

Keywords: *Climate Change, Growing Season, Downscaling, Iran.*

Riassunto: *Questo studio affronta l'impatto del riscaldamento globale sui cambiamenti spazio-temporali della stagione di crescita in Iran nei prossimi decenni utilizzando i dati giornalieri di 43 stazioni meteorologiche presenti sul territorio nazionale durante il periodo 1981-2010. I dati per i periodi futuri sono stati simulati con LARS-WG ed.5 utilizzando gli output di due modelli di circolazione generale atmosferica (HadCM3 e GFCM21) e tre scenari di emissione (A2, B1 e A1B). L'analisi delle condizioni termiche future suggerisce un maggiore aumento della temperatura minima rispetto alla massima. Rispetto alla stagione di crescita 1981-2010, i risultati basati sul modello GFCM21 per gli scenari di emissione A2, A1B e B1 hanno mostrato che la durata della stagione di crescita nel periodo 2046-2065 verrà estesa, rispettivamente, di 21, 19 e 13 giorni. Sulla base del modello HadCM3 e degli scenari sopra citati, l'aumento medio della durata della stagione di crescita in Iran è, rispettivamente, di 18, 17 e 14 giorni. Il modello GFCM21 prevede che la stagione di crescita venga estesa di 29, 32 e 17 giorni nel periodo 2080-2099. L'estensione media della stagione vegetativa secondo il modello HadCM3 è di 28, 34 e 20 giorni rispetto al periodo di osservazione.*

Parole chiave: *Cambiamento Climatico, Stagione di Crescita, Downscaling, Iran.*

1. INTRODUCTION

The climate determines the type of agricultural products that can be cultivated in the region. Frost is one of the most important factors that affect the amount of agricultural production to a large extent. Occurring as a result of temperature drop to a critical threshold, frost will damage products if it is intense and lasts for a long time (Alijani *et al.*, 2010). Frosts are categorized into two groups based on their origin: Radiation Frost and Advection Frost. Radiation frost takes place as the surface loses heat (Geiger *et al.*, 1995) while Advection frost is a result of horizontal movement of an air mass at a sub-zero temperature (Cornford, 1938; Rogers *et al.*, 1970; Howell *et al.*, 1981). One of the statistical indicators of frosts is the length of the growing season. The growing season is also titled as the frost-free (Brown, 1976) or no-frost season (WMO[1], 1969), plant growing season and the length of the no-frost season (Alijani *et al.*, 2013).

Many definitions have been presented for the growing season length (Brown, 1976; Brinkman, 1979; Baron *et al.*, 1984; Skaggs and Baker, 1985), However, the most common of them are the definitions related to the occurrence of the first autumn frost and the last spring frost (Robeson, 2002). Moreover, different studies analyzed the characteristics of the growing season with the help of phenology (Menzel and Fabian, 1999; Schwartz and Reiter, 2000; Scheifinger *et al.*, 2003). Furthermore, growing season is defined

* Corresponding author's e-mail:p_mahmoudi@gep.usb.ac.ir
[1] Department of Climatology, Faculty of Planning and Environmental Sciences, Tabriz University, Tabriz, Iran.
[2] Department of Physical Geography, Faculty of Geography and Environmental Planning, Sistan and Baluchestan University, Zahedan, Iran.
Submitted 20 November 2017, accepted 14 September 2018.

[1] World Meteorological Organization.

DOI:10.19199/2018.3.2038-5625.015

differently for different locations and it is based on many climate variables, as the characteristics of the growing season for tropical regions are often associated with the spatial distribution of rainfall while in middle latitudes they are associated with the spatial distribution of temperature (Robinson and Henderson-Sellers , 1986).

Many researchers analyzed the trend of changes in growing season length, providing various results. Heino *et al.*, (1999) found evidence suggesting a decrease in the number of frost days in northern and central Europe from the 1930s on that matches the intense increase of the minimum winter temperature in Europe (Easterling *et al.*, 2000). Furthermore, an average of 10.8 days was added to the growing season from 1959 to 1993 (Menzel and Fabian, 1999). Trends of the extreme minimum winter temperature in China show a 2.5 °C increase during the period of 1951-1990 (Zhai *et al.*, 1999). Summer in Estonia has become significantly longer while its winter has become shorter by almost 30 days (Jaagus and Ahas, 2000). In New Zealand, the frequency of cold nights has been reduced by 10 to 20 from 1951 to 1996 (Salinger and Griffiths, 2001). Schwartz and Reiter (2000) claim that late spring frost in North America has been shifted toward the beginning of spring. However, the shift is unsteady and nonlinear. Baron *et al.*, (1984) verified that, in Massachusetts, late spring frosts are followed by earlier autumn frosts. This systematic relation was resulted from investigating data start and end of every frost from a period of 70 years.

In addition, the number of days of growing season has been reduced in the Midwestern United States since the climax of northern hemisphere warming in 1940 (Brown, 1976). Growing season in the State of Minnesota has been extended during the course of the 20th century due to the time of last early frosts and the first late frosts being shifted, but the extent of the increase was different in the studied stations (Skagges and Baker, 1985). Brinkmann (1979) showed that the growing season length in Wisconsin extended in the period of 1985-1900. Sharratt (1992) also verified that the growing season length has been extended in multiple stations during the course of the 20th century. Cooter and Leduc (1995) showed that the frost-free season starts 11 days earlier now compared to the 1950s in the northeastern United States. Furthermore, DeGaetano (1996) reported significant trends in the reduction of the number of cold extreme days across the same region. In Illinois, growing season length has been extended by almost a week in the last 100 years which is a result of early spring frosts. However, the dates of first autumn frosts have remained substantially the same (Robeson, 2002).

In addition to studies pertaining to the trend of changes in growing season length, simulations of General Circulation Models (GCMs) also predict extension of the growing season for the 21st century. Based on A1B, B1, and A2 emission scenarios, the growing season is expected to be extended by 27-42 days in Idaho State in The United States by 2099 (Santos *et al.*, 2015). Predictions based on B1 and A2 emission scenarios show that by 2050 the growing season in northern Estonia is extended by 16 to 24 days and by 18 to 28 days in the southern part of the country (Saue and Karemaa, 2015). Based on the results of GCMs outputs, the growing season length in Catskill Mountains, New York, will be extended by 10 to 25 days and by 13 to 40 days in the span of 2045-2065 and 2080-2099 respectively (Anandhi *et al.*, 2013).

In recent years, extensive studies have been conducted in Iran on climate change and its impact on the long-term behavior of minimum, maximum and average temperatures. Many of these studies verified the increasing trend in the minimum temperatures in Iran; however, it is to be noted that the trend is not the same everywhere in the country (Alijani *et al.*, 2011a). Furthermore, the spatial cores of cold waves were observed to be displaced from latitudes around 35° toward latitudes above 36° in the west and northwestern Iran (Alijani *et al.*, 2011b). Sedaghat Kerdar and Rahimzadeh (2007) also investigated the changes in growing season length during the second half of the 20th century, in 16 weather stations in Iran, based on three index extents: the number of frost days, the number of icing days and the growing season length. Their results suggest extended growing season length in most stations in the country, especially in the northern parts, with Kermanshah, Mashhad and Tehran stations being extended 12, 9 and 7 days respectively. Consequently, the above cited stations were associated with a decreasing trend in the number of frost days. In Tehran, frost days were reduced by 7, and by 4 in Isfahan, Mashhad, and Shiraz. Using Statistical downscaling models, Esmaeili *et al.*, (2010) examined the alterations of growing season and frost period length for the past (1976-2005) and future periods (2011-2040) in Mashhad, Torbat-e Heydarieh, and Sabzevar stations in

northeastern Iran. They showed that the growing season have been extended in Mashhad and Sabzevar, shortened in Torbat-e Heydarieh; the length of frost period was reduced by 15-16 days in all three stations which was attributed to global warming. The average length of growing season in Iran was 231 days during the period of 1961-2000. However, UKMO climate scenarios predict an elongation of 15 days by 2025 and 29 days by 2050 for growing season in Iran (Koocheki *et al.*, 2006). The impact of climate change on rainfed wheat production in Iran showed the shortening of the growing period as cultivation date is shifted toward winter, reducing the production in all the studied sites (Nassiri *et al.*, 2006; Roshan *et al.*, 2014).

Increasing the length of growing period causes change in hydrologic cycle by increasing evapotranspiration, more drainage of soil moisture and decreasing stream flow. These changes lead to an increase in water requirement of plants and ultimately more use of water (CCSP. 2008. Christiansen *et al.*, 2011). Investigations carried out by ElMahdi *et al.*, (2009), Gohari *et al.*, (2013) and Zamani *et al.*, (2016) in various parts of Iran suggest an increase in temperature in all months of the year for the coming decades. Moreover, agricultural water demand will increase and the region will face an increasing trend in water demand. This is of utmost importance in Iran, a country with arid and semi-arid climate and suffering from water shortage. In order to manage the impact of climate change on the agriculture sector, a precise investigation seems to be necessary. This research aims to simulate the effects of increasing the minimum temperature on the time displacement of date of the first and last occurrence of autumn and spring frosts of Iran at a temperature threshold of zero degree Celsius and less than it. These displacements cause changes in the length of the growing period, that is, time interval between the end of the frost in the spring and the beginning of the frost in the autumn. Moreover, the comparison of the mean growing period of past and future in different areas of Iran based on different scenarios of climate change is considered as the main objective of this research.

2. MATERIALS AND METHODS

This study was conducted within the framework of five stages: 1) Sift of General Circulation Model (GCM) data under various emission scenarios for Iran 2) Statistical downscaling of the GCM using the LARS-WG statistical downscaling model 3) validation of the statistical downscaling model with the help of observation data 4) prediction of the minimum temperature (T_{min}) corresponding to climate change scenarios for the next 85 years (ex. 2011-2030 (2025), 2046-2065 (2055) and 2080-2099 (2085)) and 5) extraction of the growing season length for observation and future periods based on predefined thresholds and by comparing them with one another. The studied region, data, models, and methods are explained in the following sections.

2.1. Study area

With a total area of 1 648 195 square kilometers, the vast country of Iran is located between geographical latitudes 25 to 40 northern degree and longitude 44 to 63 eastern degree in desert belt of northern hemisphere. Owing to special geographical location and topography characteristics of each region of Iran, different climates govern it. The mean annual precipitation in Iran is approximately 250 mm and 73% of its area has precipitation less than 300 mm and 5.7% of it has precipitation more than 550 mm. The air temperature in Iran depends on altitude, latitude and moisture sources. In this regard, the effect of altitude on air temperature is more than other parameters. The governance of planetary conditions also has a significant impact on temperature changes in Iran. For example, the governance of the subtropical high pressure in the warm season, especially in southern latitudes and governance of Siberian high pressure in the cold season, especially in the north-east, have significant impact on Iran's climate. All of the mentioned conditions have caused Iran to have a warm climate with mid-latitude continental temperature regimen. Considering the temporal-spatial scale of this research, January with 6.3 degree Celsius is the coldest month of the year and July with 29.8 degree Celsius is the warmest month of the year in Iran. More than 78 percent of Iran's area experiences mean temperature of more than 15 degree Celsius in year, and the warmest region of Iran is south and southeast and the coldest region is northwest. The mean temperature of Iran increases from north to south and from west to east, which increase in the temperature in the western-eastern direction is due to the mountains and topography of west of Iran and increase in temperature in northern-southern direction is due to approaching the

equator and increasing the angle of sun and the moisture richness of atmosphere in the aquatic zones in south of Iran (Masoodian, 2009).

2.2. Data

The data required for the research comprises two groups of observation and simulated data. The observation data (Fig. 1) from Iran Meteorological Organization, are a complete set of information including the minimum and maximum temperatures, precipitation and daily sun hours from 43 synoptic stations in various parts of Iran spanning a period of 30 years (1981-2010). The data were processed for generating simulated data for the future. The second group is the simulated data of future period (2025s, 2055s and 2085s) generated using the downscaled output of large-scale general circulation models (GCMs) in LARS-WG model (version 5) under the emission scenarios (B1, A2, A1B).

2.3. Methods

2.3.1. LARS-WG model

In order to downscale the output of large-scale general circulation models (GCMs), one of the most well-known stochastic weather generator models called as Long Ashton research station weather generator (Lars-WG) was used. This model is used to generate precipitation, solar radiation, and single-site maximum and minimum daily temperatures under both current and future climate conditions (Semenov *et al.*, 1998) The original version of LARS-WG was first introduced in 1990 as part of the Assessment of Agricultural Risk Project in Hungary. The efficiency of the LARS-WG model was evaluated and approved by Semenov in 1990 at 18 meteorological stations in the United States, Europe and Asia (Babaeian and Najafi, 2011).

LARS-WG is based on the series weather generator described in Racsko *et al.*, (1991). It utilizes semi-empirical distributions for the lengths of wet and dry day series, daily precipitation and daily solar radiation. The semi-empirical distribution $Emp = \{a_0, a_i; h_i, i = 1,..., 10\}$ is a histogram with ten intervals, $[a_{i-1}, a_i]$, where $a_{i-1} < a_i$, and h_i denotes the number of events from the observed data in the i-th interval. Random values from the semi-empirical distributions are chosen by first selecting one of the intervals (using the proportion of events in each interval as the selection probability), and then selecting a value within that interval from the uniform distribution. Such a distribution is flexible and can approximate a wide variety of shapes by adjusting the intervals

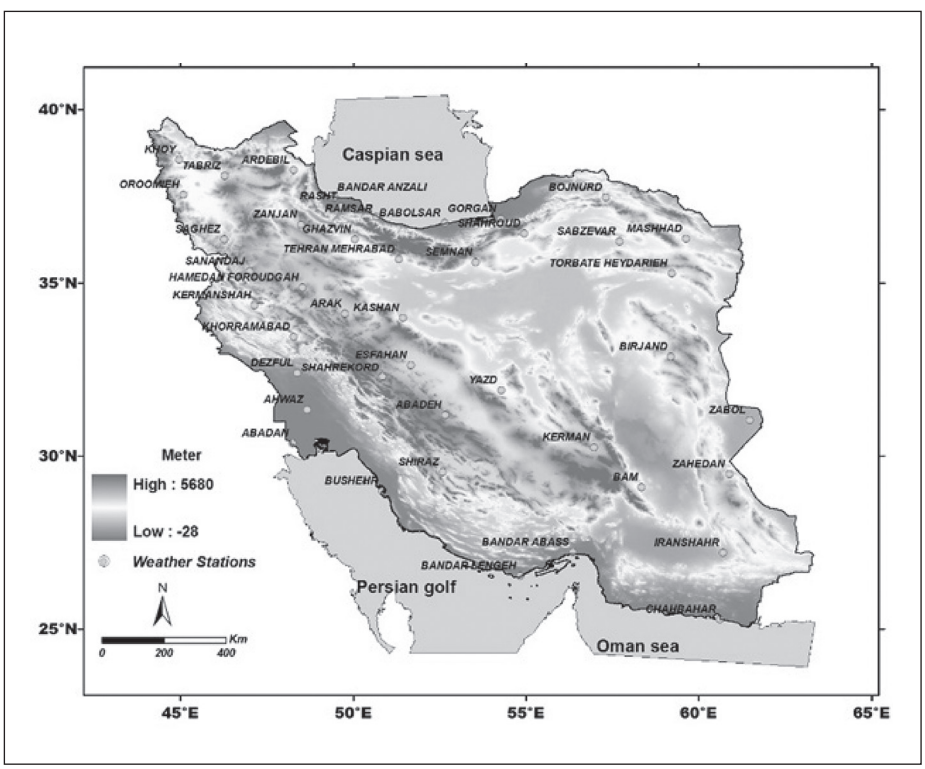

Fig. 1 - A map of the weather stations located in Iran used in this study.
Fig. 1 - Mappa delle stazioni meteo localizzate sul territorio iraniano utilizzate in questo studio.

$[a_{i-1}, a_i]$. The cost of this flexibility, however, is that the distribution requires 21 parameters (11 values denoting the interval bounds and 10 values indicating the number of events within each interval) to be specified compared with, for example, 3 parameters for the mixed-exponential distribution used in an earlier version of the model to define the dry and wet day series (Racsko *et al.*, 1991).
Daily minimum and maximum temperatures are considered as stochastic processes with daily means and daily standard deviations conditioned on the wet or dry status of the day. The technique used to simulate the process is very similar to that presented in Racsko *et al.*, (1991). The seasonal cycles of means and standard deviations are modelled by finite Fourier series of order 3 and the residuals are approximated by a normal distribution. The Fourier series for the mean is fitted to the observed mean values for each month. Before fitting the standard deviation Fourier series, the observed standard deviations for each month are adjusted to give an estimated average daily standard deviation by removing the estimated effect of the changes in the mean within the month. The adjustment is calculated using the fitted Fourier series already obtained for the mean.
The observed residuals, obtained by removing the fitted mean value from the observed data, are used to analyse a time autocorrelation for minimum and maximum temperatures. For simplicity both of these are assumed to be constant through the whole year for both dry and wet days with the average value from the observed data being used. Minimum and maximum temperature residuals have a pre-set cross- correlation of 0.6. Occasionally, simulated minimum temperature is greater than simulated maximum temperature, in which case the program replaces the minimum temperature by the maximum less 0.1 (Semenov and Barrow, 2002).
In LARS-WG, the process of generating synthetic weather data can be divided into three distinct steps, *Model Calibration, Model Validation, and Generation of Synthetic Weather Data,* which are briefly described as follows. More detailed description of the modeling procedure can be referred to Semenov (2002).

2.3.1.1. Model calibration
Model calibration is done to use the function "SITE ANALYSIS" in LARS-WG, which analyzes observed weather data (e.g., precipitation and the maximum and minimum temperature) to determine their statistical characteristics and stores this information in two parameter files.

2.3.1.2. Model Validation
The parameter files derived from observed weather data during the model calibration process are used to generate synthetic weather data having the same statistical characteristics as the original observed data. Model validation is to analyze and compare the statistical characteristics of the observed and synthetic weather data to assess the ability of LARS-WG to simulate the precipitation, Tmax, and Tmin at the chosen sites in order to determine whether or not it is suitable for use in the study. In order to evaluate whether the probability distribution in the generated data is close to that in observation data from the studied stations, the probability distribution of observation and simulated data were evaluated by the Q-Test option using the K-S goodness-of-fit test (Kolmogorov-Smirnov) with the average and standard deviation of the data being evaluated by paired sample T (T-dependent) test, and their level of significance at 0.05.

2.3.1.3. Generation of Synthetic Weather Data
The parameter files derived from observed weather data during the model calibration process can also be used to generate synthetic data corresponding to a particular climate change scenario simulated by GCMs (Chen *et al.*, 2013).

2.3.2. Confidence intervals
In simulations related to climate change studies, it is not always possible to include all the factors affecting the studied variable. Thus, the outputs of these simulations are always associated with some error or uncertainty. Thus, recognizing these errors or uncertainties in the simulations of each model seems to be necessary in making judgments and ensuring the output of the results. Hence, this research examined output uncertainty of the two selected models using Bootstrap method and in monthly base.
In the Bootstrap method, it is assumed that $X = (x_1, x_2, ..., x_n)$ is a random sample of the unknown distribution of population F. It is also assumed that the statistic of interest $\theta = t\ (F)$ is estimated using X sample. First, the statistic of interest is calculated from B size. In the next step, the standard deviation and significance level are used to determine the confidence interval. Taking these two values account, statistics on interest of

previous step are fitted to the normal distribution in the previous step, and the two upper and lower limits are determined in accordance with significance level. In this study, the simulated values of the two selected models for the minimum temperature variable and at each station were used as bootstrap input. In addition, Bootstrap output would be uncertainty band of selected models' output at 99% significance level. The 99% uncertainty band means that if the given variable is fitted in the normal distribution, with probability of 99%, values of this variable are placed in the range of 0.5 and 99.5%. In other words, if the estimated values of the models are within the confidence interval of the observed data, it indicates the significance at the desired level, and if it is out of this interval, it indica-tes the uncertainty to the estimated value. To obtain more information on the details of this method, you can refer to the references of Erfon and Tibshirani (2014) and DiCiccio and Erfon (1996).

2.4. Global climate models

In the LARS-WG pre-assumption, there are 15 general circulation models (GCMs) under the emission scenarios (B1, A2, A1B). To select the most suitable model among the 15 existing models, it is necessary that their performance and efficiency to be evaluated and approved in simulation of future data. The most suitable model is selected based on the maximum value of the coefficient of determination (R^2) (Bozorgnia and Khorami, 2007), the minimum value of Root-Mean-Square Error (RMSE) (Bozorgnia and Khorami, 2007) and the maximum value of Willmott's index of agreement (d) (Willmott *et al.*, 2011), which their value is always between zero and one. In this index, the value 1 indicates the best fit, and the zero value indicates the worst fit. The equations related to coefficient of determination, root-mean-square error, and Willmott's index of agreement (equations 1 to 3) are presented below:

$$R^2 = \frac{\frac{1}{2}\left[\sum_{i=1}^{n}(Xi - \overline{X})(Yi - \overline{Y})\right]}{\sum_{i=1}^{n}(Xi - \overline{X})^2 \sum_{i=1}^{n}(Yi - \overline{Y})^2} \quad (1)$$

In this equation, the value of R^2 represents a linear relationship between simulated and observed data, which its value is between 0 and 1. As this value is closer to 1, the linear relationship between the two values would be stronger. *Xi* and *Yi* represent the simulated and observed ith data and $\overline{X}$ and $\overline{Y}$ are the mean of the total data.

$$RMSE = \frac{1}{n}\sqrt{\sum_{n=1}^{n}(Sim, i - obs, i)^2} \quad (2)$$

$$d = 1 - \left\{\frac{\sum_{i=1}^{n}(|Sim, i - obs, i|)^2}{\sum_{i=1}^{n}(|Simi - \overline{obs}| + |obs, i - \overline{obsi}|)^2}\right\} \quad (3)$$

In these equations, *sim*, *i* is simulated values, $\overline{obs}$, *i* is observed value, andi is the mean observed values. Finally, from the 15-model set of Lars models, two global climates models (GFCM21 and HADCM3) with maximum efficiency (correlation) and the minimum simulation error in estimating the temperature parameter were selected as models to examine the effect of climate change on growing period in Iran.

2.4.1. HadCM3 model

The output of HadCM3 (Hadley GCM3) was used for this research. This model uses 360-day year and incorporates a spatial grid of 2.5° latitude and 3.75° longitude. The General Circulation Model (GCM) consists of a complex model of earth surface processes including: 1) 23 categories of vegetation. 2) 4 layers of soil where temperature, frost, and ice melting are traced. 3) and an accurate evaporation and condensation function which depends on temperature, partial pressure of water vapor, type of vegetation and concentration of atmosphere carbon dioxide. This model is known to be one of the most complete of GCMs. HadCM3 is a unique GCM that do not require flux adjustment in order to generate a real scenario (Gordon *et al.*, 2000).

2.4.2. GFCM21 model

This is one of the models by Geophysical Fluid Dynamics Laboratory of the Princeton University, which is designed for atmospheric and ocean climate simulation in a daily time scale. The atmospheric model ed. CM2.1 offers a resolution of 2*2.5° (latitude*longitude) and 24 vertical levels. The ocean model with a resolution of 1*1° (latitude*longitude) has 50 vertical levels (Delworth et al, 2006). Model simulations predict the Thermohaline circulation to be reduced. Thermohaline, also known as the global ocean conveyor belt, is especially important; since the circulation is accountable for the transport of a

large portion of the heat from tropical regions to higher latitudes in the current climate (Shamsipour, 2013).
Any change in the concentration of greenhouse gases in the atmosphere results in an imbalance between components of the earth climate system. But it is not certainly determined how much of such gases entered the atmosphere as a result of human activity and how they will impact the climate on earth. Therefore, the predictions are presented with uncertainty and for various scenarios. Data simulated with the two aforementioned models for the time periods of 2046-2065 and 2088-2099 were implemented for A2, A1B, and B1 emission scenarios. The characteristics of the selected scenarios are presented in Tab. 1. After forming a database of minimum observed and simulated temperature data, the length of the growing season, that is, the number of days between the last spring frost and the first autumn frost (zero temperature and less) was individually extracted for each station. Next, the growing season length of observation and simulated data were compared and growing season length variation maps were generated based on the observation data reported by the stations.

3. RESULTS AND DISCUSSION

3.1. Validation of LARS WG

Examining LARS validation results, it was found that the k-s test was significant and acceptable for all stations. The T-test was also significant at a level of 0.05 in all stations except for Bojnourd in the month of JUN, Bushehr and Shahr-e Kord in MAR, Isfahan in FEB and Zahedan in AUG. Overall, it is safe to say that LARS-WG is well capable of simulating the minimum temperatures of the studied stations in Iran with random error.

3.2. Analysis of uncertainty

For example, the uncertainty analysis related to the mean temperature of the Sanandaj Meteorological Station is presented in Fig. 2. The results of the analysis for this station indicate that the mean of monthly minimum temperature of Sanandaj Station is in the confidence interval of 99% for 10 months and its standard deviation is in the confidence interval of 99% only for 2 months, and rest of months are out of this interval. However, the results for all of the studied stations revealed that mean minimum temperature of 72.7% of months and standard deviation of only 6.6% of the months were in the 99% confidence interval (their diagrams have not been illustrated). Thus, the results suggest the weakness of the model in the estimation of standard deviation. Two models and three scenarios were used to reduce this uncertainty, as stated before.

3.3. The trend of minimum and maximum temperatures of Iran

Investigating the trend of long-term changes in mean annual minimum and maximum

Description	Scenario
The A1B scenario describes a future world of very rapid economic growth, low population growth, and the rapid introduction of new and more efficient technologies, with a balanced emphasis on all energy sources. Major underlying themes are convergence among regions, capacity building, and increased cultural and social interactions, with a substantial reduction in regional differences in per capita income.	A1B
The A2 storyline and scenario family describes a very heterogeneous world. The underlying theme is self-reliance and preservation of local identities. Fertility patterns across regions converge very slowly, which results in continuously increasing population. Economic development is primarily regionally oriented and per capita economic growth and technological change more fragmented and slower than other storylines.	A2
The B1 storyline and scenario family describes a convergent world with the same global population, that peaks in mid-century and declines thereafter, as in the A1 storyline, but with rapid change in economic structures toward a service and information economy, with reductions in material intensity and the introduction of clean and resource-efficient technologies. The emphasis is on global solutions to economic, social and environmental sustainability, including improved equity, but without additional climate initiatives.	B1

Tab. 1 - Characteristics of scenarios B1, A1B and A2 future period. (Pachauri and Reisinger, 2007).
Tab. 1 - Caratterisitche degli scenari futuri B1, A1B e A2 (Pachuari e Reisinger, 2007).

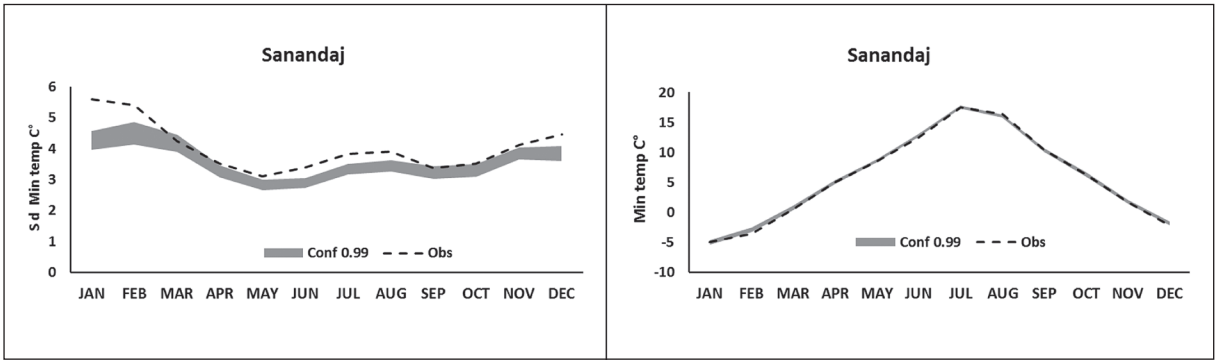

Fig. 2 - Bootstrap graph mean and minimum temperature of Sanandaj station in confidence interval 99%.
Fig. 2 - Temperatura media e minima della stazione di Sanandaj con intervallo di confidenza 99%.

temperatures of Iran in the 2020s, 2050s and 2090s compared to the base period (1981-2010) for the two HadCM3 and GFCM2 models shows that the rate of increase in minimum temperature is higher than that in maximum temperature (Tab. 2). The increase in minimum temperature has a great impact on frost indices such as frequency of frost days, the variation of the date of the first and the last frosts, frost period length, and growing season length.

3.4. Growing season length in the Period of Observation

The results of investigating the station data suggest that the mean growing period or non-frost period, that is the time interval between the last spring frost to the first autumn frost at a threshold of zero Celsius temperature and lower, is 266 days in Iran.This region is frost-free. Moving away from the coast, growing season is shortened. After the southern coastline, lowlands in south and southeast and the coast of the Caspian Sea are associated with the largest GSLs. The shortest GSL corresponds to mountainous regions of the north west-south east stations, namely: Ardabil, Saqqez, Shahr-e Kord and Hamedan stations with 164, 170, 172 and 178 days respectively (Fig. 3).

3.5. Growing season length in the Future

Compared to the growing season of 1981-2010, based on the GFCM21 model and A2, A1B and B1 emission scenarios, the length of growing season in the time span of 2046-2065 is observed to be extended by 22, 19 and 13 days respectively all across Iran. Based on the A1B scenario, stations on the shore of the Caspian Sea (Gorgan, Rasht) and also Khorramabad are associated with the maximum increase. The number of frost-free

Period	Scenario	Minimum temperature C°	Maximum temperature C°
2011-2030	A1B	0.71	0.67
	A2	0.75	0.71
	B1	0.68	0.65
2046-2065	A1B	2.37	2.34
	A2	2.16	2.13
	B1	1.8	1.68
2080-2099	A1B	3.5	3.47
	A2	4.09	4.07
	B1	2.37	2.34

Tab. 2 - The average annual increase in minimum and maximum temperatures of Iran in the decades of 20, 50 and 90 future models: HadCM3 and GFCM21, Compared with the period (1981-2010).
Tab. 2 - Aumento medio annuo delle temperature minime e massime in Iran nei decenni futuri 20, 50 e 90 secondo i modelli HadCM3 e GFCM21, rispetto al periodo (1981-2010).

stations will reach 11. This means growing season length will be extended to 365 days all across the coastline of the Persian Gulf and the Oman Sea, and in lowlands of the southeast, and at stations on the northern coastline, namely Bandar-e Anzali, Babolsar, and Ramsar. In A2 and B1 scenarios, spatial changes are similar to those for the A1B scenario. Tabriz, Arak, Qazvin, Urumia, Khoy and Sanandaj stations in northwestern Iran will be impacted the least, and Gorgan, Rasht, Khorramabad stations will be impacted the most. Based on the HadCM3 model and the aforementioned scenarios, the average increase in the growing season in Iran is 18, 17 and 14 days

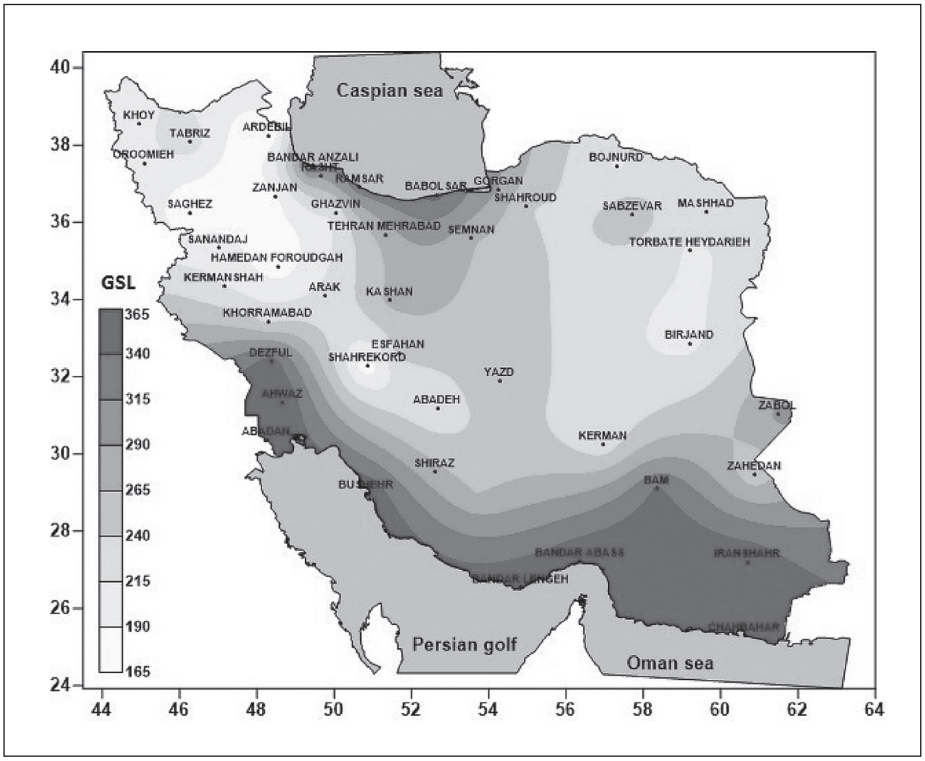

Fig. 3 - Average of growing season length during the observation period (1981-2010) in Iran.
Fig. 3 - Durata media della stagione di crescita durante il periodo di osservazione (1981-2010) in Iran.

respectively. Spatial changes of growing season length is not much different than for GFCM21 but the changes are more limited. Maximum increase will take place in Gorgan, Ramsar and Rasht on the northern coastline, Ardabil, Hamedan, Khorramabad and Shahr-e Kord in mountainous regions of the west and northwest and also in Mashhad in northeastern Iran. Yazd, Abadeh and Shiraz stations in the southern half, and Sabzevar, Semnan, Tehran, and Tabriz in the northern half of the country will be associated with the lowest increase in growing season length (Fig. 4, Tab. 3).

The GFCM21 model predicts the growing season to be extended by 29, 32 and 17 days in during the period of 2080-2099. Based on the A1B scenario, the growing season length in Gorgan and Rasht on the northern shores, Shiraz in the southern half of the country, and mountainous stations of the west and northwest, namely Ardabil, Hamedan, Saqqez, Shahr-e Kord and Khorramabad will be increased by more than 45 days compared to the period of observation. Tabriz station will be accompanied by the lowest increase. The growing season length of stations mentioned in the earlier scenario will be increased by more than 50 days in the pessimistic A2 scenario, with the lowest increase taking place, again, in Tabriz. In the optimistic B1 scenario, however, the increase will be less intense and the growing season length in the stations will be extended by 30-35 days. The average extension of growing season in HadCM3 model compared to the observed period is 28, 34 and 21 days. Based on the A1B scenario, Gorgan and Rasht stations on the coast of the Caspian Sea, and Ardabil, Khorramabad and Shahr-e Kord in the northwest and also Mashhad and Torbat-e Heydarieh will experience the highest increase in growing season length by more than 40 days compared to the period of observation. Sanandaj and Qazvin stations in the northwest, and Semnan and Sabzevar in the north-east, and Abadeh in the Southern half of Iran will be impacted the least, changing by 24-26 days. Based on the pessimistic A2 scenario, Tabriz, Arak and Qazvin stations will experience the lowest increase in growing season length, while Gorgan and Rasht on the coast of the Caspian Sea, and Ardabil, Khorramabad and Shahr-e Kord in the northwest will experience the highest increase in growing season length. In the B1 scenario, Zabol station will experience a significant increase in addition to the previously mentioned stations. The lowest increase takes place in Sabzevar, Abade and Tabriz stations (Fig. 5, Tab. 4). Investigations carried out by

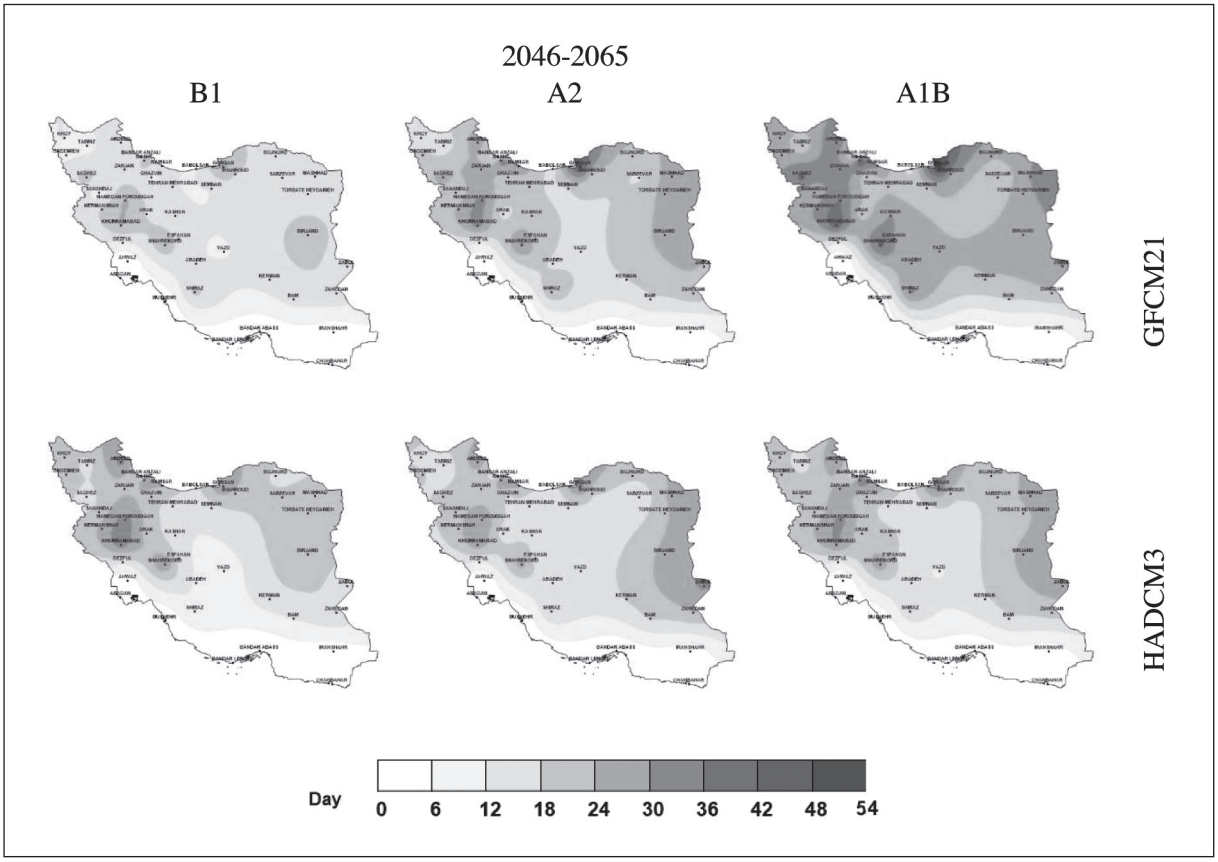

Fig. 4 - GLS changes in the period (2046-2065), based on models GFCM21 and HADCM3, under emission scenarios A1B, A2 and B1 compared with the observation period (1981-2010) in Iran.
Fig. 4 - Cambiamenti GLS nel periodo (2046-2065), basati sui modelli GFCM21 e HADCM3, sotto gli scenari di emissione A1B, A2 e B1 rispetto al periodo di osservazione (1981-2010) in Iran.

Koochaki and Kamali (2009) suggest that leaf area index and the absorbed solar radiation will be reduced compared to the current situation, in the conditions of climate change despite an increase in CO_2 concentration. Reduction in the absorption of solar radiation will reduce the growth rate of the product, resulting in the significant production of dry material. Moreover, shortage of water due to the increased evapotranspiration will reduce the rate of growth. Their prediction suggests reduction in production of rainfed wheat by 16-24% in 2025 and 22-32% in 2050.

4. CONCLUSIONS

In this research, the outputs of two general circulation models (HadCM3 and GFCM21) under three emission scenarios (A2, A1B, and B1) were downscaled on 43 synoptic stations in Iran. The results suggest the minimum temperature will be increased to a larger extent compared to the maximum temperature in the following decades in Iran. The increase of the minimum temperature changes frost indices such as growing season length, being the number of days between the last spring frost and the first autumn frost (0°C and below). Compared to the period of 1981-2010, the results based on the GFCM21 model for A2, A1B, and B1 emission scenarios show the length of growing season in the span of 2046-2065 to be extended by 21, 19 and 13 days respectively. Based on the HadCM3 model and the aforementioned scenarios, the average increase in the growing season in Iran is 18, 17 and 14 days respectively. The GFCM21 model predicts the growing season to be extended by 29, 32 and 17 days in during the period of 2080-2099. The average extension of growing season in HadCM3 model compared to the observed period is 28, 34 and 20 days. The results of the present study are in agreement with previous studies carried out in other parts of the world suggesting an increase in the length of growing season in Iran. However, the extent of

STATION	growing season length 1981-2010	Differences in growth period simulated (2046-2065) with observations					
		GFCM21			HADCM3		
		A1B	A2	B1	A1B	A2	B1
KHOY	210	28	16	12	19	18	16
TABRIZ	228	19	13	9	15	13	13
ARDEBIL	164	36	27	18	29	28	27
OROOMIEH	211	26	19	10	23	19	20
BANDAR ANZALI	354	10	11	10	11	11	10
RASHT	293	43	33	23	36	31	24
BOJNURD	212	25	21	12	18	19	14
SAGHEZ	170	38	27	21	24	19	13
ZANJAN	186	33	26	15	24	20	19
GHAZVIN	221	19	18	11	18	17	16
RAMSAR	333	31	31	15	30	25	21
BABOLSAR	349	16	16	12	16	15	14
GORGAN	290	52	46	26	35	33	25
SHAHROUD	242	29	22	18	19	19	18
SABZEVAR	256	18	17	13	20	13	16
MASHHAD	224	30	27	13	27	26	15
SANANDAJ	206	23	18	8	18	20	16
TEHRAN	276	24	20	12	17	14	13
SEMNAN	269	22	18	12	16	15	13
TORBATE	212	28	27	15	22	23	18
KERMANSHAH	215	3.2	25	19	25	22	22
HAMEDAN	178	36	32	25	32	30	27
ARAK	224	20	15	17	20	15	18
KHORRAMABAD	235	42	33	25	31	28	28
KASHAN	272	30	22	14	19	17	12
DEZFUL	354	11	11	11	11	11	11
SHAHREKORD	172	39	31	23	29	27	25
ESFAHAN	248	29	21	15	18	15	12
BIRJAND	209	27	26	21	26	26	20
AHWAZ	365	0	0	0	0	0	0
ABADEH	219	24	17	12	13	13	9
YAZD	266	24	16	11	11	14	7
ZABOL	296	30	24	14	27	31	10
ABADAN	362	3	3	3	3	3	3
KERMAN	221	23	18	15	17	18	13
SHIRAZ	274	32	23	20	17	18	10
BAM	344	18	17	14	17	18	10
ZAHEDAN	248	23	22	17	21	24	15
BUSHEHR	365	0	0	0	0	0	0
BANDAR ABASS	365	0	0	0	0	0	0
IRANSHAHR	364	1	1	1	1	1	1
BANDAR LENGEH	365	0	0	0	0	0	0
CHAHBAHAR	365	0	0	0	0	0	0
Average	266	22	19	13	18	17	14

Tab. 3 - Increase growing season length in the period (2046-2065), based on models GFCM21 and HADCM3, under emission scenarios A1B, A2 and B1. compared with the observation period (1981-2010) in Iran.
Tab. 3 - Incremento della durata della stagione di crescita nel periodo (2046-2065), sulla base dei modelli GFCM21 e HADCM, sotto gli scenari di emissione A1B, A2 e B1 rispetto al periodo di osservazione (1981-2010) in Iran.

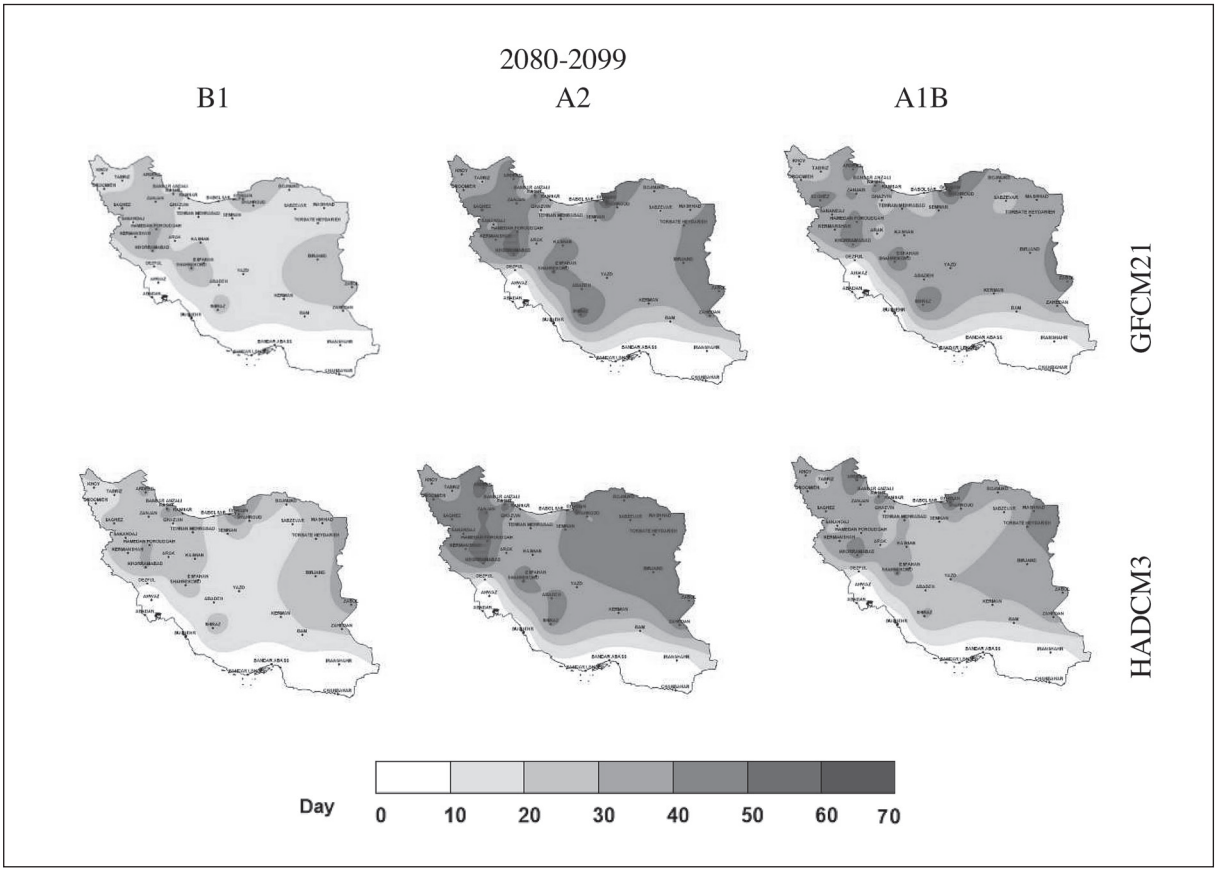

Fig. 5 - Growing season length changes in the period (2080-2099), based on models GFCM21 and HADCM3, under emission scenarios A1B, A2 and B1 compared with the observation period (1981-2010) in Iran.
Fig. 5 - Cambiamento della durata della stagione di crescita nel periodo (2080-2099), sulla base dei modelli GFCM21 e HADCM, sotto gli scenari di emissione A1B, A2 e B1 rispetto al periodo di osservazione (1981-2010) in Iran.

changes is different based on the region, climate change scenario, the general circulation model employed and the predicted period of time. The results presented here are in agreement with those reported by Nasiri *et al.*, (2007), showing an increase in the growing season length in all studied stations in Iran for the period 2025 to 2050. However, based on the A2 scenario, Kheyrandish *et al.*, (2012) predicted the growing length to be extended in Mashhad, Tehran, Isfahan, Rasht and Zahedan stations while being shortened in Tabriz, Kerman and Gorgan stations in the period of 2020-2050. Based on the B1 scenario, the aforementioned variable showed an increasing trend in Mashhad, Tehran and Rasht stations, while showing a decreasing trend in Kerman and Gorgan stations and in comparison with the past climate. Esmaeili *et al.*, (2010) claimed growing season to be extended in Mashhad and Sabzevar stations and shortened in Torbat-e Heydarieh station in the future.

Elongation of growing season through increased evaporation and condensation, loss of moisture in the soil and poor transport, change the hydrological cycle and results in a larger water demand by plants hence greater water consumption. This is of utmost importance in Iran, a country with arid and semi-arid climate and suffering from water shortage. The results of this study can help economic and social planners identify the impact of climate change on various sectors especially agriculture, and guide the arrangements for adaptation to different climate change scenarios in Iran.

REFERENCES

Alijani B., Mahmoudi P., Rigi Chahi A. B., Khosravi P., 2010. Investigation of the persistence of frost days in Iran using Markov Chain Model. Physical Geography Research Quarterly, 73: 1-20. (In Persian)

Alijani B., Salighe M., Mahmoudi P., Rigi Chahi

STATION	growing season length 1981-2010	Differences in growth period simulated (2080-2099) with observations					
		GFCM21			HADCM3		
		A1B	A2	B1	A1B	A2	B1
KHOY	210	29	33	18	32	38	20
TABRIZ	228	21	28	12	26	32	17
ARDEBIL	164	47	50	30	52	57	33
OROOMIEH	211	30	37	19	34	42	20
BANDAR ANZALI	354	11	11	10	11	11	11
RASHT	293	50	56	29	54	60	46
BOJNURD	212	35	36	19	32	43	20
SAGHEZ	170	48	51	31	40	48	22
ZANJAN	186	40	45	25	38	51	28
GHAZVIN	221	25	27	17	24	29	18
RAMSAR	333	32	32	18	32	32	31
BABOLSAR	349	16	16	14	16	16	16
GORGAN	290	65	65	32	55	56	51
SHAHROUD	242	37	38	22	32	40	22
SABZEVAR	256	26	29	13	25	40	16
MASHHAD	224	34	38	15	41	47	29
SANANDAJ	206	29	36	18	24	39	24
TEHRAN	276	32	34	15	33	39	23
SEMNAN	269	31	38	12	26	43	20
TORBAT	212	38	41	18	41	47	26
KERMANSHAH	215	37	46	24	37	50	25
HAMEDAN	178	44	51	34	39	54	32
ARAK	224	26	29	15	29	30	20
KHORRAMABAD	235	49	58	32	47	53	32
KASHAN	272	40	44	21	30	38	22
DEZFUL	354	11	11	11	11	11	11
SHAHREKORD	172	49	53	33	43	53	28
ESFAHAN	248	38	39	21	29	36	19
BIRJAND	209	38	41	25	35	46	27
AHWAZ	365	0	0	0	0	0	0
ABADEH	219	36	41	18	25	40	17
YAZD	266	35	35	17	30	39	18
ZABOL	296	42	45	21	40	49	34
ABADAN	362	3	3	3	3	3	3
KERMAN	221	31	32	18	29	34	18
SHIRAZ	274	50	55	23	32	43	25
BAM	344	21	21	17	20	21	18
ZAHEDAN	248	37	43	20	35	46	23
BUSHEHR	365	0	0	0	0	0	0
BANDAR ABASS	365	0	0	0	0	0	0
IRANSHAHR	364	1	1	1	1	1	1
BANDAR LENGEH	365	0	0	0	0	0	0
CHAHBAHAR	365	0	0	0	0	0	0
Average	266	29	32	17	28	34	21

Tab. 4 - Increase growing season length in the period (2080-2099), based on models GFCM21 and HADCM3, under emission scenarios A1B, A2 and B1 compared with the observation period (1981-2010) in Iran.
Tab. 4 - Incremento della durata della stagione di crescita nel periodo (2080-2099), sulla base dei modelli GFCM21 e HADCM, sotto gli scenari di emissione A1B, A2 e B1 rispetto al periodo di osservazione (1981-2010) in Iran.

AB., 2011 a. Study of annual maximum and minimum temperatures Changes in Iran. Quarterly Journal of Geographical Research, 24(98): 1-20. (In Persian)

Alijani B., Mahmoudi P., Panahi A., 2011 b. Investigation of displacement of minimum temperatures temporal and spatial cores in west and northern west of Iran. Geography and Environmental Planning (University of Isfahan), 22(1(41)): 13-16. (In Persian)

Alijani B., Mahmoudi P., Kalim D.M., 2013. New approach for determining the length of potential growing season in Iran. Journal of Water and Soil (Agricultural Sciences and Technology) 27 (5): 861-871. (In Persian)

Anandhi A., Zion MS., Gowda P.H., Pierson D.C., Lounsbury D., Frei A., 2013. Past and future changes in frost day indices in Catskill Mountain region of New York. Hydrological Processes, 27(21): 3094-3104.

Babaeian I., Najafi Z., 2011. Climate Change Assessment in Khorasan-e Razavi Province from 2010 to 2039 Using Statistical Downscaling of GCM Output. Journal Of Geography and Regional Development, 15: 1-21. (In Persian)

Baron W.R., Gordon G.A., Borns Jr H.W., Smith D.C., 1984. Frost-free record reconstruction for eastern Massachusetts, 1733-1980. Journal of climate and applied meteorology, 23(2): 317-319. http://dx.doi.org/10.1175/1520-0450(1984)023<0317:FFRRFE>2.0.CO;2

Bozorgnia A., Khorrami M., 2007. Analysis of Time Series with MINITAB1 Software, Sokhan Gostar Publishing, Mashhad, 1-333. (In Persian)

Brinkmann W., 1979. Growing season length as an indicator of climatic variations? Climatic Change, 2(2): 127-138.

Brown J.A., 1976. Shortening of growing season in the US Corn Belt. Nature, 260: 420-421.

Christiansen D.E., Markstrom S.L., Hay L.E., 2011. Impacts of climate change on the growing season in the United States. Earth Interactions, 15(33), pp.1-17. http://dx.doi.org/10.1175/2011EI376.1

CCSP., 2008. The Effects of Climate Change on Agriculture, Land Resources, Water Resources, and Biodiversity in the United States. Chapter 3: Land Resources: Forest and Arid Lands. A Report by the U.S. Climate Change Science Program and the Subcommittee on Global Change Research. Backlund P., Janetos A., Schimel D., Hatfield J., Boote K., Fay P., Hahn L., Izaurralde C., Kimball B.A., Mader T., Morgan J., Ort D., Polley W., Thomson A., Wolfe D., Ryan M., Archer S., Birdsey R., Dahm C., Heath L., Hicke J., Hollinger D., Huxman T., Okin G., Oren R., Randerson J., Schlesinger W., Lettenmaier D., Major D., Poff L., Running S., Hansen L., Inouye D., Kelly B.P., Meyerson L., Peterson B., and Shaw R. U.S. Environmental Protection Agency, Washington, DC, USA.

Chen H., Guo J., Zhang Z., Xu CY., 2013. Prediction of temperature and precipitation in Sudanand South Sudan by using LARS-WG in future. Theoretical and Applied Climatolology, 113: 363-375.

Cooter E.J., Leduc S.K., 1995. Recent frost date trends in the north-eastern USA. International Journal of Climatology, 15(1): 65-75.

Cornford C.E., 1938. Katabatic winds and the prevention of frost damage. Quarterly Journal of the Royal Meteorological Society, 64(277): 553-592.

DeGaetano A.T., 1996. Recent trends in maximum and minimum temperature threshold exceedences in the northeastern United States. Journal of Climate, 9(7): 1646-1660. http://dx.doi.org/10.1175/1520-0442(1996)009<1646:RTIMAM>2.0.CO;2

Delworth T.L., Broccoli A.J., Rosati A., Stouffer R.J., Balaji V., Beesley J.A., Cooke W.F., Dixon K.W., Dunne J., Dunne K.A., Durachta J.W., 2006. GFDL's CM2 global coupled climate models. Part I: Formulation and simulation characteristics. Journal of Climate, 19(5): 643-674. http://dx.doi.org/10.1175/JCLI3629.1

DiCiccio T.J., Efron B., 1996. Bootstrap confidence intervals. Statistical Science, 11(3): 189-228.

Easterling D.R., Evans J.L., Groisman P.Y., Karl T.R., Kunkel K.E., Ambenje P., 2000. Observed variability and trends in extreme climate events: a brief review. Bulletin of the American Meteorological Society, 81(3): 417-425. http://dx.doi.org/10.1175/1520-0477(2000)081<0417:OVATIE>2.3.CO;2

Efron B., Tibshirani R.J., 1993. An Introduction to the Bootstrap. Chapman and Hall: New York.

ElMahdi A., Shahkarami N., Morid S., Massah Bavani A., 2009. Assessing the impact of AOGCMs uncertainty on the risk of agricultural water demand caused by climate change. In 18th World IMACS/MODSIM Congress, Cairns, Australia (pp. 13-17).

Esmaeili R., Habibi Nokhandan M., Fallah Ghalhary G., 2010. The changes assessment of growth season length and freezing due to climate fluctuation, case Study: Khorasan Razavi Province. Physical Geography Research Quarterly, 73: 69-82. (In Persian)

Geiger R., Aron R., Todhunter P., 1995. The climate near the ground. Vieweg, Braunschweig, Germany, 528 pp.

Gohari A., Eslamian S., Abedi-Koupaei J., Bavani A.M., Wang D., Madani, K., 2013. Climate change impacts on crop production in Iran's Zayandeh-Rud River Basin. Science of the Total Environment, 442: 405-419. https://doi.org/10.1016/j.scitotenv.2012.10.029

Gordon C., Cooper C., Senior C.A., Banks H., Gregory J.M., Johns T.C., Mitchell J.F., Wood R.A., 2000. The simulation of SST, sea ice extents and ocean heat transports in a version of the Hadley Centre coupled model without flux adjustments. Climate dynamics, 16(2): 147-168.

Heino R., Brázdil R., Førland E., Tuomenvirta H., Alexandersson H., Beniston M., Pfister C., Rebetez M., Rosenhagen G., Rösner S., Wibig J., 1999. Progress in the study of climatic extremes in Northern and Central Europe. In Weather and Climate Extremes (pp. 151-181). Springer Netherlands.

Howell G.W., Johnson D.E., Mansfield T.K., 1981. Factors influencing spring freeze damage to developing grape shoots. Proc. Mich. Grap Soc, 2: 1-22.

Jaagus J., Ahas, R., 2000. Space-time variations of climatic seasons and their correlation with the phenological development of nature in Estonia. Climate Research, 15(3): 207-219.

Kheyrandish F., Ghahraman N., Bazrafshan J., 2012. The effects of climate change on the growing season in the 2020 and 2050 in several climatic zones of Iran. Journal of Soil and Water Research of Iran (Iranian Agricultural Sciences), 44(2): 143-150. (In Persian)

Koocheki A., Kamali G.A., (2009). Climate change and wheat in Iran. Iranian Journal of Field Crops Research, Vol. 8, No. 3, July - Aug. 2010, p. 508-520. (In Persian)

Koocheki A., Nasiri M., Kamali G.A., Shahandeh H., 2006. Potential impacts of climate change on agro climatic indicators in Iran. Arid Land Research and Management, 20(3): 245-259. (In Persian)

Masoodian A. (2009). Iran's Weather. The first edition, published by Sharia Toos, Mashhad.

Menzel A., Fabian P., 1999. Growing season extended in Europe. Nature, 397(6721): 659-659.

Nasiri M., Koocheki A., Kamali G.A., Marashi H., 2007. The effects of climate change on agricultural climate indices in Iran. Journal of Agricultural Science and Technology. 20(7): 82-71. (In Persian)

Nassiri M., Koocheki A., Kamali G.A., Shahandeh H., 2006. Potential impact of climate change on rainfed wheat production in Iran. Archives of agronomy and soil science, 52(1): 113-124. http://dx.doi.org/10.1080/03650340600560053

Pachauri R.K., Reisinger A., 2007. Contribution of working groups I, II and III to the fourth assessment report of the intergovernmental panel on climate change. IPCC, Geneva, Switzerland, 104.

Racsko P., Szeidl L., Semenov M., 1991. A serial approach to local stochastic weather models. Ecological Modelling, 57: 27-41.

Robeson S.M., 2002. Increasing growing-season length in Illinois during the 20th century. Climatic Change, 52(1): 219-238.

Robinson P.J., Henderson-Sellers A., 1999: Contemporary Climatology 2nd edition. Pearson Education Ltd, Harlow, Uk.

Rogers W.J., Swift H.L., 1970. Frost and the prevention of frost damage. US Department of Commerce NOAA, Silver Spring, MD.

Roshan G., Oji R., Al-Yahyai S., 2014. Impact of climate change on the wheat-growing season over Iran. Arabian Journal of Geosciences, 7(8): 3217-3226.

Salinger M.J., Griffiths G.M., 2001. Trends in New Zealand daily temperature and rainfall extremes. International Journal of Climatology, 21(12): 1437-1452.

Santos CACD., Rao TVR., Olinda RAD., 2015. Trends in temperature and growing season length in Idaho-USA during the past few decades. Revista Brasileira de Meteorologia, 30(4): 359-370.

Saue T., Karemma K., 2015. Lengthening of the thermal growing season duo climate change in Estonia. Towards climatic services. Nitra, Slovakia, 15th - 18th September 2015.

Scheifinger H., Menzel A., Koch E., Peter C., 2003. Trends of spring time frost events and phenological dates in Central Europe. Theoretical and Applied Climatology, 74(1-2): 41-51.

Schwartz M.D., Reiter B.E., 2000. Changes in

north American spring. International Journal of climatology, 20(8): 929-932.
Sedaghat Kerdar A.A., Rahimzadeh F., 2007. Variation of growing season length (GSL) over second half of 20th in Iran. Pajouhesh – Va-Sazandegi, in Agronomy and Horticulture), 20(2): 182-193. (In Persian)
Semenov M.A., Barrow E.M., 2002. A stochastic weather generator for use in climate impact studies. User's manual, Version, 3. http://www.rothamsted.ac.uk/masmodels/larswg.php: 1-27.
Semenov M.A., Brooks R.J., Barrow E.M., Richardson C.W., 1998. Comparison of the WGEN and LARS-WG stochastic weather generators in diverse climates. Clim Res 10:95-107.
Shamsipour A., 2013. Climate modeling Theory and Method. University of Tehran press, Tehran, Iran, 430. (In Persian)
Sharratt B.S., 1992. Growing season trends in the Alaskan climate record. Arctic, 45(2): 124-127.
Skaggs R.H., Baker D.G., 1985. Fluctuations in the length of the growing season in Minnesota. Climatic Change, 7(4): 403-414.
Willmott C.J., Robeson S.M., and Matsuura K., 2011. A refined index of model performance. International Journal of Climatology, 32 (13): 2088-2094.
WMO., 1969. Protection against frost damage. No: 133, TP60, 2-19.
Zamani R., Akhond-Ali AM., Roozbahani A., Fattahi R., 2017. Risk assessment of agricultural water requirement based on a multi-model ensemble framework, southwest of Iran. Theoretical and Applied Climatology, 129(3-4): 1109-1121.
Zhai P., Sun A., Ren F., Liu X., Gao B., Zhang Q., 1999. Changes of climate extremes in China. Climate Change, 42(1): 203-218.